Discovery of *Mycobacterium tuberculosis* CYP121 New Inhibitor via Structure-Based Drug Repurposing

Tarek El Moudaka[1,2], Priya Murugan[2], Mohd Basyaruddin Abdul Rahman[2] and Bimo Ario Tejo[2]*

[1]*Department of Biotechnology, Faculty of Applied Sciences, UCSI University, No. 1 Jalan Menara Gading, Cheras, Malaysia*
[2]*Department of Chemistry, Faculty of Science, Universiti Putra Malaysia, 43400 UPM, Serdang, Malaysia*

ABSTRACT

Tuberculosis (TB) remains a serious threat to human health with the advent of multi-drug resistant tuberculosis (MDR-TB) and extensively drug-resistant tuberculosis (XDR-TB). The urge to find novel drugs to deal with the appearance of drug-resistant TB and its variants is highly needed. This study aims to find new CYP121 inhibitors by screening 8,773 compounds from the drug repositioning database RepoDB. The selection of CYP121 potential inhibitors was based on two criteria: the new inhibitor should bind to CYP121 with higher affinity than its original ligand and interact with catalytically important residues for the function of CYP121. The ligands were docked onto CYP121 using AutoDock Vina, and the molecular dynamics simulation of the selected ligand was conducted using YASARA Structure. We found that antrafenine, an anti-inflammatory and analgesic agent with high CYP inhibitory promiscuity, was bound to CYP121 with a binding affinity of -12.6 kcal/mol and interacted with important residues at the CYP121 binding site. Molecular dynamics analysis of CYP121 bound to the original ligand and antrafenine showed that both ligands affected the dynamics of residues located distantly from the active site. Antrafenine caused more structural changes to CYP121 than the original ligand, as indicated by a significantly higher number of affected residues and rigid body movements caused by the binding of antrafenine to CYP121.

Keywords: CYP121, drug repositioning, drug resistance, molecular docking, molecular dynamics, tuberculosis, virtual screening

INTRODUCTION

Finding an effective treatment and control of tuberculosis (TB) remains a global challenge due to the emergence of new strains of *Mycobacterium tuberculosis* expressing resistance to the present generation of drugs. TB is an infectious disease that continues to impose risks on public health, as it has infected over ten million of the population globally, of which 1,500,000 cases have resulted in death (WHO, 2019).

In humans, *M. tuberculosis* generally attacks the lungs of the infected, followed by symptoms of persistent cough, fever, hemoptysis, hyperhidrosis, and weight loss (CDC, 2019). *M. tuberculosis* from TB patients can infect a healthy person via airborne. When a person with TB coughs or sneezes, the disease can spread through the air, as *M. tuberculosis* is contained in aerosols (Saleem & Azher, 2013). Ultimately, a single patient suffering from TB may infect up to 15 healthy people upon being continuously in direct contact for a year (Kanabus, 2020).

Every year, approximately ten million people are infected with TB worldwide. People from middle and low-income countries such as India, Bangladesh, Indonesia, China, Nigeria, Philippines, Pakistan, and South Africa were mostly affected by TB infection in 2019 (WHO, 2020). Meanwhile, TB made a comeback in Europe recently when there was an increase in the number of cases. In Paris, for example, the numbers rose from 14.6 per 100,000 inhabitants in 2016 to 15.8 per 100,000 in 2017 due to many migrants from countries with high incidences and increased TB cases in Eastern Europe (Silue et al., 2019).

There has been a rising demand for renewed efforts in researching this devastating disease as the world is confronting a new crisis due to multidrug-resistant (MDR) and extensively drug-resistant (XDR) strains of *M. tuberculosis*. The standard treatment options for TB are no longer effective, mainly contributing to the growing spread of these MDR and XDR bacteria. The *M. tuberculosis* pathogens that have developed resistance can adapt to the TB drugs by altering their cell structures, thereby rendering the effectiveness of these drugs useless (Singh et al., 2020).

One of the emerging targets for anti-tuberculosis drugs is CYP121, a member of the cytochrome P450 family that is only found in *M. tuberculosis* (de Montellano, 2018). This enzyme is considered the most promising anti-TB drug target among other *M. tuberculosis* CYPs due to its prominent substrate specificity. CYP121 significantly binds only cyclodityrosine (cYY) with a conserved 2,5-diketopiperazine (DKP) ring carrying two aryl side chains in l-configuration. CYP121 does not efficiently or selectively transform other cYY analogs, indicating a high specificity for cYY (Fonvielle et al., 2013). Phylogenetic analysis shows that CYP121 is unique to *M. tuberculosis* with limited similarity (≤34% protein sequence identity) to other *M. tuberculosis* P450s (Belin et al., 2009), which could be attributed to the role of this enzyme in catalyzing the C–C bond-forming reaction that is not required by other bacteria (Hudson et al., 2012).

This study aims to identify new CYP121 inhibitors by virtual screening of repurposed drugs. Over eight thousand compounds from a repurposed drug database, RepoDB, were virtually screened to discover the most potential antituberculosis inhibitors. We found that antrafenine, a piperazine derivative and an analgesic anti-inflammatory drug with high CYP inhibitory promiscuity, binds to CYP121 stronger than its respective original inhibitor. Further study using molecular dynamics simulation showed that antrafenine changes the dynamics of residues located distantly from the active site of CYP121. Antrafenine can be further tested to confirm its inhibitory activity against *M. tuberculosis*.

METHODOLOGY

Software

BIOVIA Discovery Studio Visualizer (Dassault Systèmes Biovia) was utilized to visualize and modify the receptor and ligand structure and post-docking interaction analysis. Molecular format conversion was done using OpenBabel (O'Boyle et al., 2011). Molecular docking was conducted using AutoDock Vina (Trott & Olson, 2010). AutoDock Tools (Morris et al., 2009) was used to prepare the *pdbqt* files of protein and ligands. YASARA Structure software (Krieger et al., 2002) was used for molecular dynamics simulation.

CYP121 Structure Preparation

The CYP121 structure in complex with ligand 69M was downloaded from the RCSB Protein Data Bank (PDB ID: 5IBE) (http://www.rcsb.org/). The crystal structure was set up for molecular docking by eliminating all water molecules and sulfate ions using BIOVIA Discovery Studio Visualizer. Ligand 69M was separated from the protein structure and saved as a *.pdbqt* file.

Preparation of Ligand Structures

The three-dimensional structures of 8,773 drug molecules were downloaded from the RepoDB database (http://apps.chiragjpgroup.org/repoDB/) in *.sdf* format (Brown & Patel, 2017). All the drug molecules in the RepoDB database were linked to the DrugBank database (https://go.drugbank.com/) (Wishart et al., 2018). A specific ID number was used to identify the molecular compounds used in this work. All 8,773 ligands were converted to *.pdbqt* file format for molecular docking.

Molecular Docking

Molecular docking was performed using AutoDock Vina. AutoDock Tools was used to create the *.pdbqt* input file for CYP121 and set the size and center of the grid box. Polar hydrogen atoms and Kollman charges were set for CYP121. The validation step

to determine the docking parameters was conducted by re-docking the original ligand of CYP121 (69M) into its respective binding site. The ligand 69M was removed from the CYP121 crystal structure and prepared for re-docking by adding polar hydrogen and partial charges, then saved as a *.pdbqt* file. The center of the grid box and box size was varied until the re-docked conformation of ligand 69M matched its crystal structure. Based on the validation step result, the grid box's center was set to -7.612 × 18.984 × 4.466 (x, y, z) using 1.000 Å spacing and a box size of 40 × 40 × 40. The predicted binding affinity (kcal/mol) was calculated using the AutoDock Vina scoring function. BIOVIA Discovery Studio Visualizer was used to analyze the docking results.

ADMET Prediction

Toxtree (http://toxtree.sourceforge.net/predict/) and SWISSADME (http://swissadme.ch/) were employed to determine the toxicological and pharmacological properties of the ligands. The analyzed properties were carcinogenicity, mutagenicity, AMES test, Lipinski's rule of five for drug-likeness, and corrosive properties. The CYP450 inhibitory promiscuity of each ligand was determined using admetSAR as implemented in the DrugBank database (http://lmmd.ecust.edu.cn/admetsar2/) (Cheng et al., 2012).

Molecular Dynamics

Molecular dynamics simulations were conducted using YASARA Structure on a Windows 10 computer. The AMBER03 force field implemented in YASARA Structure was used in the simulation. The Ewald particle algorithm was used to calculate the long-distance Coulomb interactions. The van der Waals force was set to 8 Å. A hexahedral box of 50 x 50 x 50 Å size was placed around the protein. The water density was fixed to 1 g / mL at a temperature of 298 K. The periodic boundary condition (PBC) was set for the simulated box. The simulation was conducted for 50 ns with trajectories saved every 100 ps. Molecular dynamics outputs were analyzed using *md_analyze.mcr* and *md_analyzeres.mcr* macros implemented in YASARA Structure. The protein domain movement was analyzed using the DynDom program (http://dyndom.cmp.uea.ac.uk/dyndom/ runDyndom.jsp) (Hayward & Berendsen, 1998).

RESULTS AND DISCUSSION

Tuberculosis (TB) has emerged as a significant health issue, and a concern in many nations due to the existence of multidrug-resistant (MDR) and, more recently, extensively drug-resistant (XDR) strains of *M. tuberculosis* (Ouellet et al., 2010). The extensive spread of drug-resistant TB creates a threatening scenario with only a 30% success rate in the treatment (Bhat et al., 2018). Current treatments are becoming complicated by the increasing

number of resistant strains of *M. tuberculosis*, which has led to the urgency to discover new drugs to treat TB disease (Lockart et al., 2020).

The latest recommended treatment available for TB includes isoniazid, rifampicin, pyrazinamide, and ethambutol for the first two months. For the next four months, isoniazid and rifampicin drugs are needed for treatment. MDR-TB is resistant to first-line TB drugs such as isoniazid and rifampicin, whereas XDR-TB is highly resistant to second-line TB drugs. Meanwhile, drug-resistant tuberculosis (TDR-TB) is resistant to a wide range of first-line and second-line drugs (Reddyrajula et al., 2019).

The resistance of bacterial strains to the first-line and second-line drugs and antibiotics is mainly due to the thick, hydrophobic cell envelope and the presence of enzymes that deteriorate and alter the drugs (Gygli et al., 2017). The treatment given to the drug-resistant bacterial strain is strenuous and requires at least 6−9 months of constant therapy in ideal circumstances (Hoagland et al., 2016). Besides that, the treatment is considered more expensive, highly toxic, and requires sophisticated facilities and equipment for drug-resistant testing (Hoagland et al., 2016).

Several potential TB drugs have been approved and tested in clinical trials (Reddyrajula et al., 2019). Bedaquiline and diaryl quinoline-based molecules were approved by the US Food and Drug Agency (FDA) and the European Medicines Agency (EMA) to treat adult MDR-TB. Bedaquiline causes side effects such as cardiac arrhythmias (Reddyrajula et al., 2019). Therefore, there is an urgent need to discover new drugs targeting new receptors to combat MDR-TB and XDR-TB.

The cytochrome P450 is a superfamily of the monooxygenase enzymes having the β-heme and protoforfirin IX groups as the heme cofactor (Leys et al., 2003). In bacteria, cytochrome P450 functions in xenobiotic degradation, nitric oxide reduction, antibiotic synthesis, and fatty acid metabolism (Bogaert et al., 2010), whereas in humans, the cytochrome P450 functions in the metabolism of various drugs (Nerbert et al., 2013). Cytochrome P450 CYP121 is essential for the viability of *M. tuberculosis*, as it catalyzes the formation of mycocyclosin by forming a C-C bond between the two tyrosyl side chains of the cyclodityrosine (cYY, cyclo-L-Tyr-L-Tyr) (Ugalde et al., 2020).

The emphasis on CYP121's importance is due to its strong affinity for azole molecules and its analogs used as very effective antimycobacterial compounds for *M. tuberculosis* growth inhibition (Ahmad et al., 2005). Most azole antifungals, however, are incompatible as scaffolds for front-line oral anti-TB drug candidates due to their poor bioavailability and non-specific affinity for human CYPs, resulting in severe systemic toxicology and induced drug-drug interaction. Furthermore, azole-resistant *M. tuberculosis* mutants with up-regulation of a transmembrane transporter protein thought to function as an azole efflux pump have been isolated. (Hudson et al., 2012), which highlights the need for finding molecules other than azole drugs to bind to CYP121.

This work discovered potential inhibitors against the *M. tuberculosis* CYP121 drug target by docking a large database of molecules from the RepoDB database. The molecule compounds in the repositioning drug database (RepoDB) have been approved to treat various diseases. More than 8,000 molecules were docked into the binding site of the CYP121 crystal structure using the AutoDock Vina program. The binding affinity calculation for all 8,773 molecular compounds was determined by AutoDock Vina using a specific implemented algorithm and scoring function in the program. This study used CYP121's original ligand (69M) as a control ligand in molecular docking.

Validation of Docking Parameters

A validation step was conducted to ensure that the docking parameters allowed ligands to adopt correct conformations in the binding pocket. The original ligand (69M) was re-docked into the CYP121 crystal structure for validation docking. Our result shows that the re-docked 69M inhibitor adopted a similar conformation with its crystal structure with a binding affinity of -11.7 kcal/mol (Figure 1).

Ligand 69M was stabilized by three hydrogen bonds, i.e., between Ser237 and N25 nitrogen atoms of the ligand, between Val228 and O1 oxygen atom of the ligand, and another hydrogen bond between Thr77 and N11 nitrogen atom of the ligand. The heme group formed a pi-pi interaction with the aromatic ring of the ligand. A pi-pi stacking interaction was formed between Trp182 and Phe168 with the aryl alcohol ring of the ligand. Ala167 and Ala233 formed a pi-alkyl interaction with two aromatic ligand rings. A pi-sigma interaction was observed between Val78 and the imidazole ring of the ligand. It is interesting to note that the residues interacting with ligand 69M involve the same residues anchoring cyclodipeptide cYY ligand to CYP121, i.e., Met62, Val78, Val83, Asn85, Phe168, Trp182, Ala233, Ser237, Phe280, Gln385, Arg386, and heme group (Belin et al., 2009).
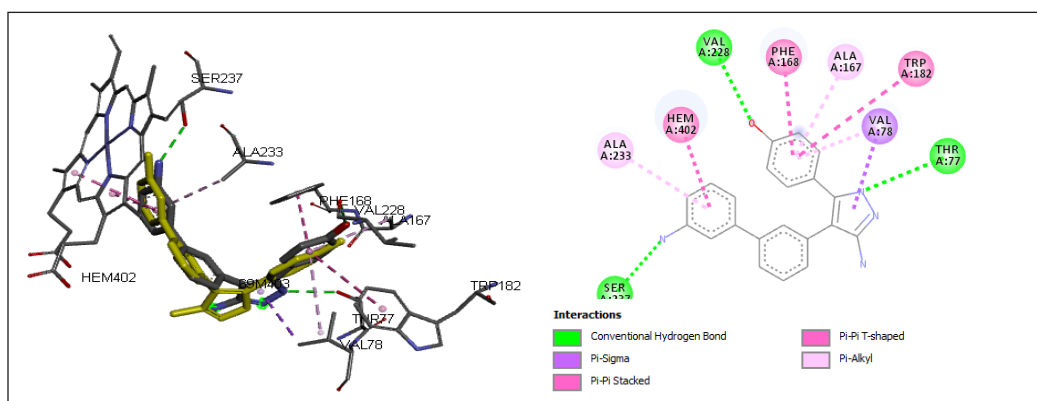

Figure 1. The redocked ligand 69M (grey) in comparison to its original position and conformation (yellow). A two-dimensional interaction map shows the types of interaction between ligand 69M and its surrounding residues.

Molecular Docking of Drug Compounds

The molecular docking of 8,773 drug compounds from the RepoDB database was carried out using the AutoDock Vina program. In order to find the potential inhibitors for *M. tuberculosis* CYP121, the compounds should have a higher binding affinity to CYP121 than that of the original ligand 69M, i.e., -11.7 kcal/mol. The top 10 docked compounds with higher binding affinity values than ligand 69M were displayed (Table 1).

Table 1
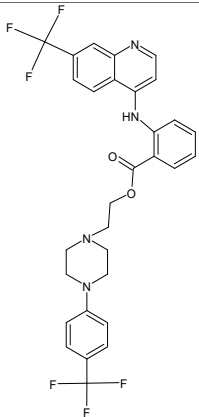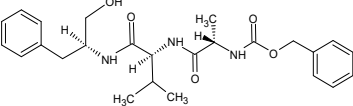*Top 10 drugs with the highest docking binding affinity to CYP121*

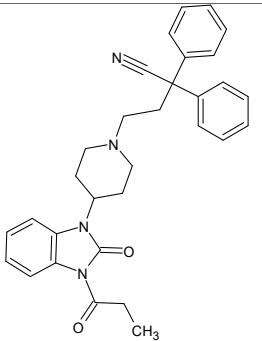| Compound ID	Drug name	Affinity (kcal/mol)	CYP inhibitory promiscuity	Molecular structure
DB04098	Balanol	-13.0	Low	
DB03992	3-(Benzoylamino)-L-alanine	-13.0	Low	
DB01419	Antrafenine	-12.6	High	
DB01891	Tl-3-093	-12.5	Low	
DB05861	Tasquinimod	-12.5	Low	
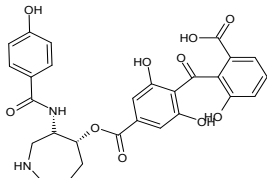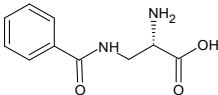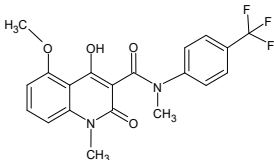
Table 1 *(continue)*
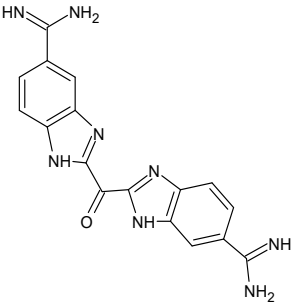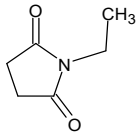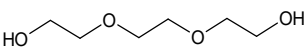
Compound ID	Drug name	Affinity (kcal/mol)	CYP inhibitory promiscuity	Molecular structure
DB05855	Rivanicline	-12.4	Low	
DB01459	Bezitramide	-12.3	Low	
DB01876	Bis(5-amidino-2-benzimidazolyl) methanone	-12.2	High	
DB01902	1-Ethyl-pyrrolidine-2,5-dione	-12.1	Low	
DB02327	Triethylene glycol	-11.9	Low	
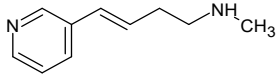
The toxicological and pharmacological properties of the top ten drugs were determined using Toxtree and SWISSADME (Table 2). All drugs used in this work were taken from RepoDB, a repurposed drug database. Therefore, we did not expect the compounds used in this work to be toxic or pharmacologically unfavorable. Toxtree and SWISSADME analysis showed that the top ten compounds were noncarcinogenic and nonmutagenic. All compounds passed the ADME test and were non-corrosive to skin, except triethylene glycol. Five compounds violated Lipinski's rule of five; however, these compounds could be formulated to improve their absorption and permeation in the later stages of drug development.

Table 2

Toxicological and pharmacological properties of the top 10 drugs with the highest docking binding affinity to CYP121

	Benigni/Bossa rules			Lipinski's rule of five		
Ligand	Carcinogenicity	Mutagenicity	AMES test	Violation	Druglikeness	Skin corrosive
Balanol	Noncarcinogenic	Nonmutagenic	Pass	3	Yes	No
3-(Benzoylamino)-L-alanine	Noncarcinogenic	Nonmutagenic	Pass	3	Yes	No
Antrafenine	Noncarcinogenic	Nonmutagenic	Pass	2	No	No
T1-3-093	Noncarcinogenic	Nonmutagenic	Pass	0	Yes	No
Tasquinimod	Noncarcinogenic	Nonmutagenic	Pass	0	Yes	No
Rivanicline	Noncarcinogenic	Nonmutagenic	Pass	0	Yes	No
Bezitramide	Noncarcinogenic	Nonmutagenic	Pass	1	Yes	No
Bis(5-amidino-2-benzimidazolyl)methanone	Noncarcinogenic	Nonmutagenic	Pass	1	Yes	No
1-ethyl-pyrrolidine-2,5-dione	Noncarcinogenic	Nonmutagenic	Pass	0	Yes	Unknown
Triethylene glycol	Noncarcinogenic	Nonmutagenic	Pass	0	Yes	Yes

Balanol (DB04098) and 3-(benzoylamino)-L-alanine (DB03992) were the highest-ranked compounds with a binding affinity of -13.0 kcal/mol. However, both compounds had low promiscuity in inhibiting cytochrome P450. Interestingly, the second-ranked compound, i.e., antrafenine (DB01419) with a binding affinity of -12.6 kcal/mol, was predicted to have high cytochrome P450 inhibitory promiscuity. The fluorine atoms attached to C25 and C42 carbon atoms of antrafenine formed hydrogen bonds with Arg386, which plays an important role in CYP121 catalytic activity (Belin et al., 2009). Furthermore, two hydrogen bonds were formed between Gln385 and Thr77 with an O8 oxygen atom of antrafenine. The aromatic ring next to the O8 oxygen atom interacted with three different residues as it formed a pi-sigma interaction with Val78, a pi-pi stacked interaction with Phe168, and a pi-alkyl bonding with Ala167.

It is important to note that antrafenine formed four interactions with the heme group, in which pi-alkyl and pi-pi interactions occurred between the heme group and quinoline ring antrafenine, also pi-alkyl and halogen interactions between fluorine of antrafenine and the heme group (Figure 2). Of 12 CYP121 residues interacting with antrafenine, six (Val78, Phe168, Phe280, Gln385, Arg386, and heme) are involved in the binding of cyclodipeptide cYY and CYP121 (Belin et al., 2009).

Antrafenine formed multiple non-covalent interactions with the heme functional group, which is important in the CYP121 catalytic activity (McLean et al., 2008; Belin et al., 2009). Among these interactions are pi-pi stacking, which stabilizes the non-covalent

contact between the aromatic rings of the heme group and antrafenine via London dispersion forces and electrostatics (Brylinski, 2018), pi-alkyl interaction, which is weaker than pi-pi stacking and dominated by London dispersion forces (Ribas et al., 2002), as well as halogen bonding which is essential for an accurate molecular interaction prediction (Li et al., 2016) and stabilizes the non-covalent interaction between a protein and a ligand (Suárez-Castro et al., 2018).

Antrafenine is a piperazine derivative and acts as an anti-inflammatory drug with high CYP inhibitory promiscuity, specifically for CYP1A2, CYP2C9, CYP2C19, and CYP3A4. Antrafenine is an analgesic agent for the relief of mild to moderate pain (Lv et al., 2020). Antrafenine targets the prostaglandin G/H synthase-1 (COX-1) and prostaglandin G/H synthase-2 (COX-2) in the cyclooxygenase pathway. The inhibition of COX-2 by antrafenine is presumably responsible for its anti-inflammatory activity. However, inhibition of COX-1 by antrafenine may be responsible for its toxicity. Further use of antrafenine as a repurposed anti-TB drug requires its dose to be adjusted to balance the risks and benefits.
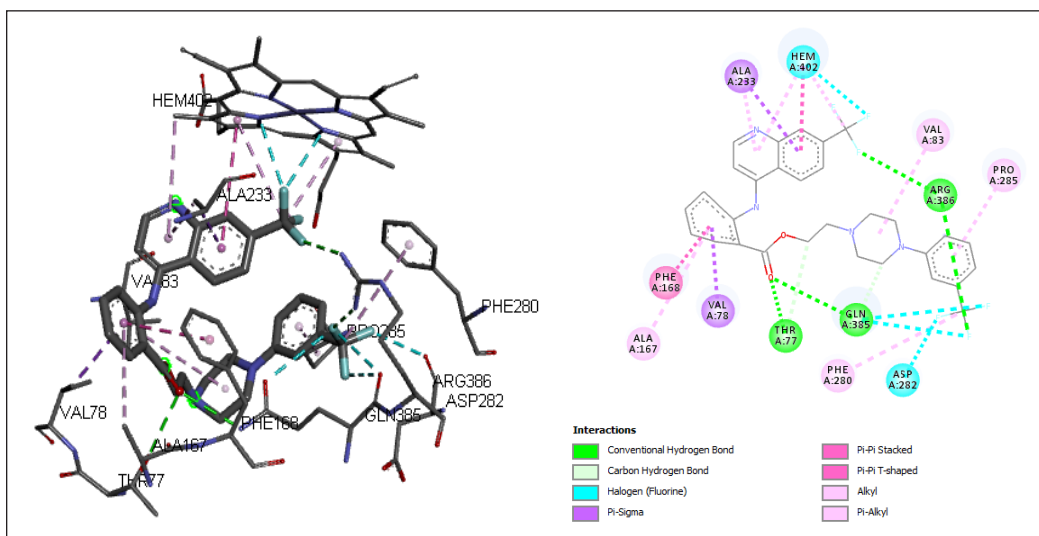

Figure 2. Antrafenine and its interactions with the surrounding amino acid residues

Molecular Dynamics

Molecular dynamics simulations were conducted to study the effect of ligands on the structure and dynamics of protein receptors. Molecular docking is typically performed on the rigid structure of the protein receptor, which does not represent a realistic condition. Molecular dynamics simulation provides a more realistic picture, where the interactions between ligand and protein receptor are optimized through conformational adjustment of the ligand and receptor after docking. Therefore, the combination of molecular docking and molecular dynamics simulation is appropriate for studying the ligand-receptor binding

mechanism and the impact of ligand binding on the structure and dynamics of receptors (Santos et al., 2019). This research used YASARA Structure to simulate the molecular dynamics of three different systems. i.e., CYP121 with no ligand (code: CYP), CYP121 in complex with ligand 69M (code: 69M), and CYP121 in complex with antrafenine (code: ANT).

The deviation of the simulated trajectory from the crystallographic structure was monitored by calculating the root-mean-square deviation (RMSD) as a function of time. RMSD compares the conformation of the protein system at a certain time to the conformation of the protein at the initial time ($t = 0$). Analysis of molecular dynamics trajectories is usually conducted when the system has reached equilibrium, i.e., when the RMSD plot has plateaued. RMSD also provides information on how far the conformational changes of the protein with the presence of the ligand are compared to those without the presence of the ligand.

The RMSD plot of the CYP system (protein without ligand) achieved a plateau earlier than that of protein with ligands, i.e., at 10 ns. The RMSD plot of the 69M system (protein with ligand 69M) reached a plateau at 20 ns. Meanwhile, the RMSD plot of the ANT system (protein with antrafenine) reached a plateau at 25 ns (Figure 3). In the CYP system, the RMSD at the equilibrium ranged between 1.4–1.7 Å. In the 69M system, the RMSD at the equilibrium ranged between 1.5–1.9 Å. Meanwhile, in the ANT system, the RMSD at the equilibrium ranged between 2.0–2.5 Å. Interestingly, the presence of antrafenine caused the CYP121 protein to have a higher deviation from its crystal structure, as indicated by the higher RMSD of ANT systems than that of the CYP and 69M systems. The difference was prominent beyond 25 ns of simulation time, where the protein in the ANT system was 2.0–2.5 Å away from its initial structure.
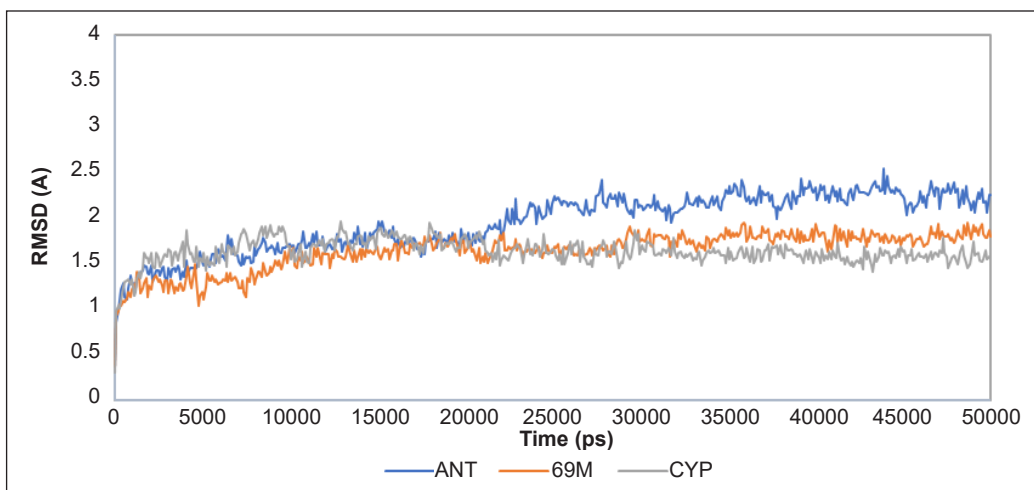

Figure 3. Root mean square deviation (RMSD) of three simulation systems (CYP, 69M, and ANT) over 50 ns of MD simulation

Analysis of CYP121 fluctuations was done by calculating the root-mean-square fluctuations (RMSF) of each residue. The RMSF values of the protein backbone in the presence of ligands, i.e., 69M and ANT systems, were compared to the RMSF values of protein without ligands, i.e., CYP system. A comparison of the RMSF values between the three systems was conducted to see the impact of ligands on the dynamics of residues in proteins. A ligand at the protein binding site impacts the dynamics of nearby residues and residues far from the binding site.

The comparison of the RMSF of the 69M and CYP systems shows that there were 17 residues in the 69M system whose RMSF were at least 50% higher than those of their values in the CYP system (Table 3 and Figure 4a). The largest change in the RMSF of the 69M system was observed at residue Phe280 with an increase of more than 100% than its value in the CYP system. On the other hand, Ala92 showed significantly lower RMSF in the 69M system, with a more than 50% drop compared to its value in the CYP system. The location of residues whose RMSF was increased by more than 50% due to the presence of ligand 69M are shown in red (Figure 4b). Interestingly, of 17 amino acid residues whose RMSF values were increased upon binding to ligand 69M, only three residues, i.e., Arg72, Ile102, and Phe230, had direct contact with ligand 69M. Fourteen residues did not interact directly with ligand 69M, indicating the long-range effect of ligand binding.

The comparison of the RMSF of the ANT and CYP systems shows that there were 61 residues in the ANT system whose RMSF were at least 50% higher than those of their values in the CYP system (Table 3 and Figure 5a). Of these 61 residues, 20 residues had

Table 3

List of residues in the 69M and ANT systems whose RMSF values are greater than 50% of their values in the CYP system

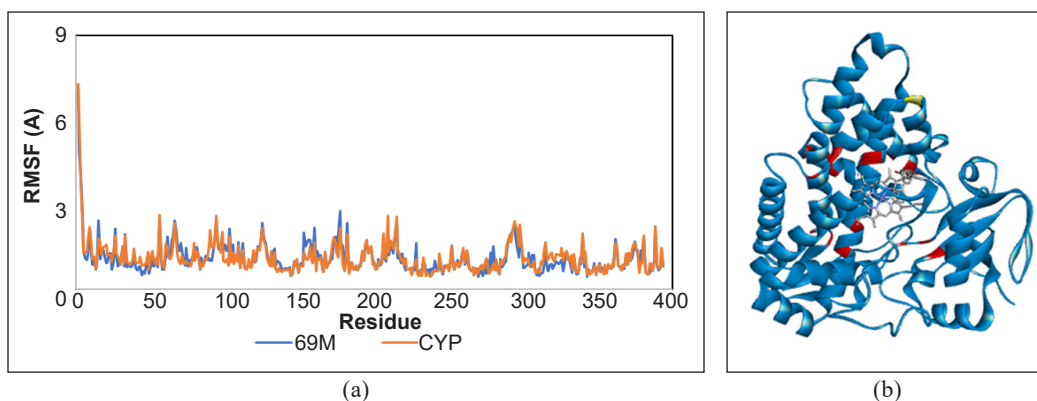| System	Residues	RMSF value
69M	Arg72, Ile102, Pro104, Arg134, Phe137, Glu155, Gly157, Pro158, Ala178, Asn181, Phe230, Ser240, Thr243, Phe280, Asp282, Leu308, Leu306	≥ 50% of their values in the CYP system
	Phe280	≥ 100% of their values in the CYP system
ANT	Arg72, Ala75, Leu76, Val82, Ala101, Pro104, Cys147, Ile152, Pro153, Gln154, Glu155, Pro158, Lys159, Leu160, Phe161, Arg162, Ser163, Leu164, Ser165, Ile166, Phe168, Ser170, Ser171, Ala172, Pro174, Pro176, Ala177, Ala178, Ile180, Asn181, Trp182, Asp183, Arg184, Asp185, Ile186, Glu187, Tyr188, Met189, Ala190, Gly191, Ile192, Leu193, Asn195, Met203, Leu206, Gly227, Val228, Phe231, Gly232, Ala233, Gly234, Ser237, Ser240, Phe280, Gln323, His354, Gln356, Gln385	≥ 50% of their values in the CYP system
	Arg28, Gly151 and Arg353	≥ 100% of their values in the CYP system

(a)   (b)

Figure 4. (a) Root mean square fluctuation (RMSF) of CYP (blue) and 69M (red) systems; and (b) Residues in the 69M system, whose RMSF values were increased by 50% and more, are shown in red.
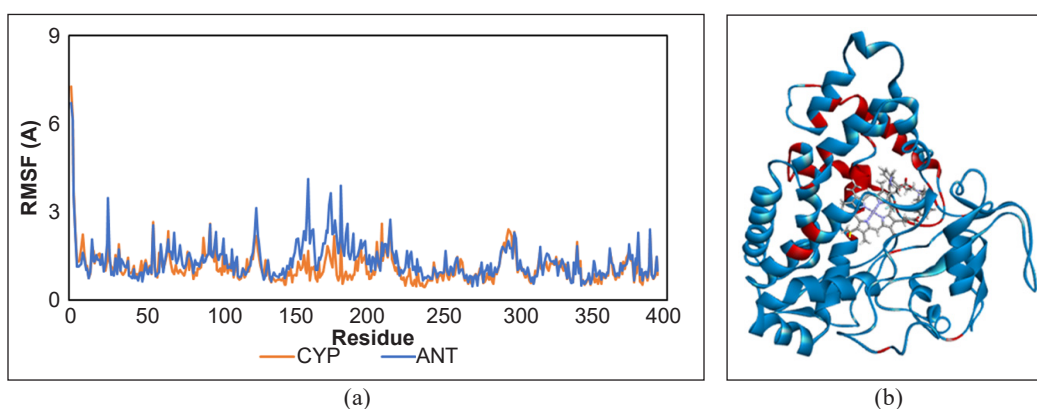

(a)   (b)

Figure 5. (a) Root mean square fluctuation (RMSF) of CYP (blue) and ANT (red) systems; and (b) Residues in the ANT system, whose RMSF values were increased by 50 % and more, are shown in red.

their RMSF increase more than 100% compared to their values in the CYP system, i.e., Arg72, Gln154, Phe161, Arg162, Ser163, Leu164, Ser165, Asn181, Trp182, Asp183, Asp185, Glu187, Tyr188, Gly191, Ile192, Met203, Gly227, Val228, Gly232 and Ser 237. The location of residues whose RMSF was increased by more than 50% due to the presence of ligand ANT is shown in red (Figure 5b). Interestingly, of 61 amino acid residues whose RMSF was increased upon binding to ANT ligand, only 10 residues, i.e., Arg72, Val82, Leu164, Phe168, Trp182, Gly232, Ala233, Ser237, Phe280, and Gln385 had direct contacts with ligand ANT. Fifty-one residues did not interact directly with ligand ANT, indicating the long-range effect of ligand binding.

Analysis of protein domain movement was carried out using DynDom, which uses the K-means clustering algorithm to find clusters of rotation vectors. DynDom analysis on the CYP system trajectory (simulated CYP121 protein without ligand) showed no rigid body movement during 50 ns of MD simulation. Similarly, for the 69M system, which was a

simulation that included the 69M ligand at the binding site of the CYP121 protein, no rigid body movement was observed during 50 ns of MD simulation. Interestingly, for the ANT system, which simulated ANT ligand with CYP121 protein, rigid body movements were observed in four segments, i.e., residues 77−80, 85−95, 164−196, and 209−228. The rigid movements of the four segments were assisted by six "hinges" (Figure 6 and Table 4). In these four moving segments, there were 12 residues whose RMSF values were more than 100% higher than their RMSF in the absence of ligand, i.e., Leu164, Ser165, Asn181, Trp182, Asp183, Asp185, Glu187, Tyr188, Gly191, Ile19, Gly227 and Val228.
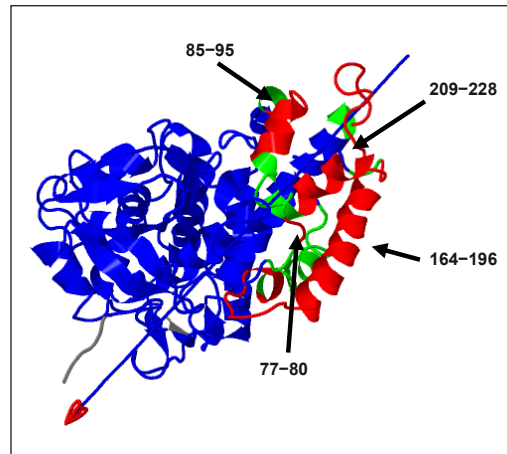

Figure 6. DynDom domain movement analysis of CYP121 in complex with ligand ANT. The fixed domains are colored blue, the moving domains are red, and the hinge domains are green. The locations of four moving domains are labeled. The arrow indicates the hinge axis. The figure was taken from DynDom output.

Table 4
List of residues that are classified as fixed (blue), moving (red), and hinge (green) in Figure 6

Domain	Residues
Fixed (blue)	6–76, 81–84, 96–163, 197–208, 229–394
Moving (red)	77–80, 85–95, 164–196, 209–228
Hinge (green)	76–77, 80–85, 95–96, 152–164, 196–197, 207–209, 228–229

Based on the DynDom dynamic contact analysis, there are four modes of domain movements in the structure of CYP121 in complex with ligand ANT, i.e., "maintained," "exchanged-partner," "exchanged-pair," and "new" (Figure 7a) (Taylor et al., 2013). The dynamic contact graph or DCG (Figure 7b) showed there were seven "maintained" (anchored) domain movements that happened between residues Thr38 → Ala172, Ala75 → Ser171, Ala75 → Pro174, Ala75 → Ile175, Ile192 → Met203, Asn195 → Ile198, and Met189 → Met203. Six "new" (open-closed) domain movements happened between residues Met86 → Val98, Met86 → Met99, Met86 → His343, Met86 → Pro346, and Lys63 → Gly87. There were two "exchanged-partner" (sliding-twist) domain movements that happened between residues Ala75 → Asp173 → Arg72 and Ala75 → Asp173 → Thr38. There were four "exchanged-pair" (see-saw) domain movements that happened between residues Ala75 → Asp173 and Pro174 → Ala75, Ala75 → Pro174 and Ser171 → Ala75, Ala75 → Ser171 and Ile175 → Ala75, Ile198 → Ile192 and Asn195 → Ile198 (Figure 7b). The four domain movements occurred only at residue segments 85−95 and 164−196,

which indicated the higher complexity of movements in these two segments. Meanwhile, the other two residue segments (77−80 and 209−228) moved freely by not following any of the four modes of domain movements.

Our results show that ligands 69M and ANT binding cause dynamic structural changes in the CYP121 protein. Most residues affected by ligands are far from the protein binding site. The long-range effect, which refers to changes in the dynamics of residues far from the binding site, is presumably caused by a "domino effect" (Oelschlaeger et al., 2003). Perturbations cause the domino effect in the residues around the ligand, which are transferred to the adjacent residues and then forwarded to the next residues. One example of a domino effect mechanism is elaborated by Stahl and Sieber (2017) using protease caseinolytic peptidase P (ClpP) as a model. The structural analysis of crystal structures of LmClpP isoforms (LmClpP1 and LmClp2) shows alterations in the amino acid arrangement within the active site and ring-ring interface. The presence of substrate in the active site seems important for the activated state. Structural x-ray analysis reveals that the

(a)

(b)

Figure 7. Dynamic contact analysis of CYP121 in complex with ligand ANT: (a) Types of domain movement and their number of instances; and (b) Dynamic contact graph (DCG) between residues in the fixed domain (blue) and moving domain (red) of CYP121. The definitions of each domain movement and elemental dynamic contact graphs (DCGs) are described in Taylor et al. (2013).

domino effect resulting in an active ClpP is caused by the transfer of binding information from the apical surface into the ClpP core. The interaction of ClpX leads to changes in the conformation of Tyr63, which seems to start at the adjacent residue Met31. It would cause Asn42 to move flexibly, exchanging its hydrogen interaction from Tyr21 to Gly33 and Asn65 and eventually resulting in conformational changes in the receptor.

Prasasty et al. (2020) recently reported the prediction of inhibitory activity of natural compounds isolated from Rhoeo spatheca and Pluchea indica against M. tuberculosis CYP121. They observed that the original ligand GGJ caused changes in the flexibility of residues at the binding site and distant residues. However, the natural compound (KAE)
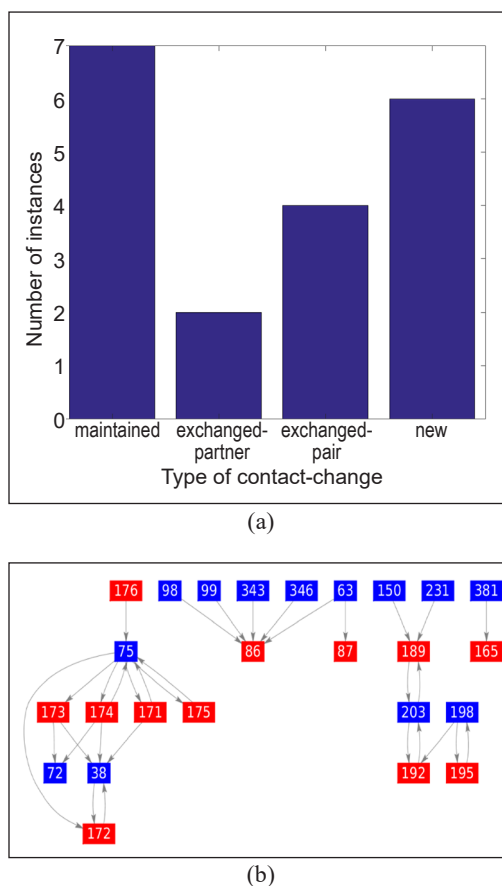
and its derivative (KAE3) did not cause any changes in the flexibility of distant residues. Our results show that the original ligand 69M changed the flexibility of distant residues, which concurs with the finding by Prasasty et al. (2020) that the long-range effect seems to play a major role in the binding mechanism of CYP121 inhibitors.

CONCLUSION

We have found antrafenine, an anti-inflammatory drug with high promiscuity to inhibit cytochrome P450, as a potential inhibitor for *M. tuberculosis* CYP121. Antrafenine, which emerged as the top CYP121 binder after docking 8,773 compounds from the RepoDB drug repositioning database, is bound to CYP121 with a binding affinity of -12.6 kcal/mol and interacts with important residues at the CYP121 binding site. Upon binding to CYP121, antrafenine affects the dynamics of residues located distantly from the active site. Our finding warrants further investigation by testing the inhibitory activity of antrafenine against *M. tuberculosis* CYP121.

ACKNOWLEDGEMENTS

REFERENCES

Ahmad, Z., Sharma, S., & Khuller, G.K. (2005). In vitro and ex vivo antimycobacterial potential of azole drugs against Mycobacterium tuberculosis H37Rv. *Federation of European Microbiological Societies Microbiology Letters, 251*(1), 19-22. https://doi.org/10.1016/j.femsle.2005.07.022

Belin, P., Le Du, M., Fielding, A., Lequin, O., Jacquet, M., Charbonnier, J., Lecoq, A., Thai, R., Courçon, M., Masson, C., Dugave, C., Genet, R., Pernodet, J., & Gondry, M. (2009). Identification and structural basis of the reaction catalyzed by CYP121, an essential cytochrome P450 in *Mycobacterium tuberculosis*. *Proceedings of the National Academy of Sciences, 106*(18), 7426-7431. https://doi.org/10.1073/pnas.0812191106

Bhat, Z. S., Rather, M. A., Maqbool, M., & Ahmad, Z. (2018). Drug targets exploited in Mycobacterium tuberculosis: Pitfalls and promises on the horizon. *Biomedicine and Pharmacotherapy, 103*, 1733-1747. https://doi.org/10.1016/j.biopha.2018.04.176

Bogaert, I. N., Groeneboer, A. V., Saerens, S. K., & Soetaert, W. (2010). The role of cytochrome P450 monooxygenases in microbial fatty acid metabolism. *The Federation of European Biochemical Societies Frequency Journal*, *278*(2), 206-221. https://doi.org/10.1111/j.1742-4658.2010.07949.x

Brown, A. S., & Patel, C. J. (2017). A standard database for drug repositioning. *Scientific Data, 4*(1), Article 170029. https://doi.org/10.1038/sdata.2017.29

Brylinski, M. (2018). Aromatic interactions at the ligand–protein interface: Implications for the development of docking scoring functions. *Chemical Biology and Drug Design*, *91*(2), 380-390. https://doi.org/10.1111/cbdd.13084

CDC. (2019). *Infectious Disease Related to Travel*. CDC. https://wwwnc.cdc.gov/travel/yellowbook/2020/travel-related-infectious-diseases/tuberculosis

Cheng, F., Li, W., Zhou, Y., Shen, J., Wu, Z., Liu, G., Lee, P. W., & Tang, Y. (2012). admetSAR: A comprehensive source and free tool for evaluating chemical ADMET properties. *Journal of Chemical Information and Modeling, 52*(11), 3099-3105. https://doi.org/10.1021/ci300367a

de Montellano, P. R. O. (2018). Potential drug targets in the Mycobacterium tuberculosis cytochrome P450 system. *Journal of Inorganic Biochemistry*, *180*, 235-245. https://doi.org/10.1016/j.jinorgbio.2018.01.010

Fonvielle, M., Le Du, M. H., Lequin, O., Lecoq, A., Jacquet, M., Thai, R., Dubois, S., Grach, G., Gondry, M., & Belin, P. (2013). Substrate and reaction specificity of Mycobacterium tuberculosis cytochrome P450 CYP121: Insights from biochemical studies and crystal structures. *Journal of Biological Chemistry*, *288*(24), 17347-17359. https://doi.org/10.1074/jbc.M112.443853

Gygli, S. M., Borrell, S., Trauner, A., & Gagneux, S. (2017). Antimicrobial resistance in Mycobacterium tuberculosis: Mechanistic and evolutionary perspectives. *Federation of European Microbiological Societies Microbiology Reviews*, *41*(30, 354-373. https://doi.org/10.1093/femsre/fux011

Hayward, S., & Berendsen, H. J. C. (1998). Systematic analysis of domain motions in proteins from conformational change: New results on citrate synthase and T4 lysozyme. *Proteins*, *30*(2), 144-154. https://doi.org/10.1002/(SICI)1097-0134(19980201)30:2%3C144::AID-PROT4%3E3.0.CO;2-N

Hoagland, D. T., Liu, J., Lee, R. B., & Lee, R. E. (2016). New agents for the treatment of drug-resistant Mycobacterium tuberculosis. *Advanced Drug Delivery Reviews*, *102,* 55-72. https://doi.org/10.1016/j.addr.2016.04.026

Hudson, S. A., McLean, K. J., Munro, A. W., & Abell, C. (2012). Mycobacterium tuberculosis cytochrome P450 enzymes: A cohort of novel TB drug targets. *Biochemical Society Transactions, 40*(3), 573-579. https://doi.org/10.1042/BST20120062

Kanabus, A. (2020). *Information about Tuberculosis*. Tbfact.org. http://www.tbfacts.org/tb/

Krieger, E., Koraimann, G., & Vriend, G. (2002). Increasing the precision of comparative models with YASARA NOVA- A self-parameterizing force field. *Proteins: Structure, Function, and Genetics*, *47*(3), 393-402. https://doi.org/10.1002/prot.10104

Leys, D., Mowat, C. G., McLean, K. J., Richmond, A., Chapman, S. K., Walkinshaw, M. D., & Munro, A. W. (2003). Atomic structure of Mycobacterium tuberculosis CYP121 to 1.06 Å reveals novel features of cytochrome P450. *Journal of Biological Chemistry*, *278*(7), 5141-5147. https://doi.org/10.1074/jbc.M2099282200

Li, Y., Guo, B., Xu, Z., Li, B., Cai, T., Zhang, X., Yu, Y., Wang, H., Shi, J., & Zhu, W. (2016). Repositioning organohalogen drugs: A case study for identification of potent B-Raf V600E inhibitors via docking and bioassay. *Scientific Reports*, *6*(1), Article 31074. https://doi.org/10.1038/srep31074

Lockart, M. M., Butler, J. T., Mize, C .J., Fair, M. N., Cruce, A. A., Conner, K. P., Atkins, W. M., & Bowman, M. K. (2020). Multiple drug binding modes in *Mycobacterium tuberculosis* CYP51B1. *Journal of Inorganic Biochemistry*, *205,* Article 110994. https://doi.org/10.1016/j.jinorgbio.2020.110994

Lv, Y., Wang, Y., Zheng, X., & Liang, G. (2020). Reveal the interaction mechanism of five old drugs targeting VEGFR2 through computational simulations. *Journal of Molecular Graphics and Modelling*, *96*, Article 107538. https://doi.org/10.1016/j.jmgm.2020.107538

McLean, K. J., Carroll P., Lewis D., Dunford A. J., Seward H. E., Neeli R., Cheesman M. R., Marsollier L., Douglas P., Smith W. E., Rosenkrands I., Cole S. T., Leys D., Parish T., & Munro A. W. (2008). Characterization of active site structure in CYP121-A cytochrome P450 essential for viability of Mycobacterium tuberculosis H37rv. *Journal of Biological Chemistry*, *283*(48), 33406-33416. https://doi.org/10.1074/jbc.M802115200

Morris, G. M., Huey, R., Lindstrom, W., Sanner, M. F., Belew, R. K., Goodsell, D. S., & Olson, A. J. (2009). AutoDock4 and AutoDockTools4: Automated docking with selective receptor flexibility. *Journal of Computational Chemistry*, *30*(16), 2785-2791. https://doi.org/10.1002/jcc.21256

Nerbert, D. W., Wikvall, K., & Miller, W. L. (2013). Human cytochromes P450 in health and disease. *Philosophical Transactions of the Royal Society of London B: Biological Sciences*, *368*(1612), Article 20120431. https://doi.org/10.1098/rstb.2012.0431

O'Boyle, N. M., Banck, M., James, C. A., Morley, C., Vandermeersch, T., & Hutchison, G. R. (2011). Open babel: An open chemical toolbox. *Journal of Cheminformatics, 3*(1), 1-14. https://doi.org/10.1186/1758-2946-3-33

Oelschlaeger, P., Schmid, R. D., & Pleiss, J. (2003). Modeling domino effects in enzymes: Molecular basis of the substrate specificity of the bacterial metallo-β-lactamases IMP-1 and IMP-6. *Biochemistry*, *42*(30), 8945-8956. https://doi.org/10.1021/bi0300332

Ouellet, H., Johnston, J. B., & de Montellano, P. R. O. (2010). The Mycobacterium tuberculosis cytochrome P450 system. *Archives of Biochemistry and Biophysics*, *493*(1), 82-95. https://doi.org/10.1016/j.abb.2009.07.011

Prasasty, V. D., Cindana, S., Ivan, F. X., Zahroh, H., & Sinaga, E. (2020). Structure-based discovery of novel inhibitors of Mycobacterium tuberculosis CYP121 from Indonesian natural products. *Computational Biology and Chemistry, 85*, Article 107205. https://doi.org/10.1016/j.compbiolchem.2020.107205

Reddyrajula, R., Dalimba, U., & Kumar, S. M. (2019). Molecular hybridization approach for phenothiazine incorporated 1,2,3-triazole hybrids as promising antimicrobial agents: Design, synthesis, molecular docking and in silico ADME studies. *European Journal of Medicinal Chemistry*, *168*, 263-282. https://doi.org/10.1016/j.ejmech.2019.02.010

Ribas, J., Cubero, E., Luque, F. J., & Orozco, M. (2002). Theoretical study of alkyl-π and aryl-π interactions. Reconciling theory and experiment. *Journal of Organic Chemistry, 67*(20), 7057-7065. https://doi.org/10.1021/jo0201225

Saleem, A., & Azher, M. (2013). The next pandemic- tuberculosis: The oldest disease of mankind rising one more time. *British Journal of Medical Practitioners*, *6*(2), 21-46.

Suárez-Castro, A., Valle-Sánchez, M., Cortés-García, C. J., & Chacón-García, L. (2018). Molecular docking in halogen bonding. In P. Vlachakis (Ed.), *Molecular Docking* (pp. 99-112). Intechopen. http://dx.doi.org/10.5772/intechopen.72994

Santos, L. H. S., Ferreira, R. S., & Caffarena, E. R. (2019). Integrating molecular docking and molecular dynamics simulations. In W. F. de Azevedo (Ed.), *Methods in Molecular Biology* (pp. 13-34). Humana Press. https://doi.org/ 10.1007/978-1-4939-9752-7_2

Silue, Y., Lepoutre, A., Mounchetrou-Njoya, I., Lapora, S., Calba, C., & Guthmann, J. (2019). Increase of tuberculosis incidence in Ile-de-France region and the role of recent migration. *European Journal of Public Health*, *29*(Supplement_4), Article ckz186-033. https://doi.org/10.1093/eurpub/ckz186.033

Singh, R., Dwivedi, S. P., Gaharwar, U. S., Meena, R., Rajamani, P., & Prasad, T. (2020). Recent updates on drug resistance in Mycobacterium tuberculosis. *Journal of Applied Microbiology*, *128*(6), 1547-1567. https://doi.org/10.1111/jam.14478

Stahl, M., & Sieber, S. A. (2017). An amino acid domino effect orchestrates ClpP's conformational states. *Current Opinion in Chemical Biology*, *40*, 102-110. https://doi.org/10.1016/j.cbpa.2017.08.007

Taylor, D, Cawley, G., & Hayward, S. (2013). Classification of domain movements in proteins using dynamic contact graphs. *PLoS ONE*, *8*(11), Article e81224. https://doi.org/10.1371/journal.pone.0081224

Trott, O., & Olson, A. J. (2010). AutoDock Vina: Improving the speed and accuracy of docking with a new scoring function, efficient optimization and multithreading. *Journal of Computational Chemistry*, *31*(2), 455-461. https://doi.org/10.1002/jcc.21334

Ugalde, S. O., Wallraven, K., Speer, A., Bitter, W., Grossman, T. N., & Commandeur, J. N. M. (2020). Acetylene containing cyclo(L-Tyr-L-Tyr)-analogs as mechanism-based inhibitors of CYP121A1 from Mycobacterium tuberculosis. *Biochemical Pharmacology*, *177*, Article 113938. https://doi.org/10.1016/j.bcp.2020.113938

Wishart, D. S., Feunang, Y. D., Guo, A. C., Lo, E. J., Marcu, A., Grant, J. R., Sajed, T., Johnson, D., Li, C., Sayeeda, Z., Assempour, N., Iynkkaran, I., Liu, Y., Maciejewski, A., Gale, N., Wilson, A., Chin, L., Cummings, R., Le, D., Pon, A., Knox, C., & Wil, M. (2018). DrugBank 5.0: A major update to the DrugBank database for 2018. *Nucleic Acids Research*, *46*(1), 1074-1082. https://doi.org/10.1093/nar/gkx1037

WHO. (2019). *Global Tuberculosis Report 2019*. World Health Organization. https://www.who.int/publications/i/item/9789241565714

WHO. (2020). *Global tuberculosis report 2020*. World Health Organization. https://www.who.int/publications/i/item/9789240013131